Available online at www.sciencedirect.com

ScienceDirect

journal homepage: www.jfda-online.com

Original Article

The detoxifying effects of structural elements of persimmon tannin on Chinese cobra phospholipase A_2 correlated with their structural disturbing effects well

Ying Zhang [a], *Chun-Mei Li* [a,b,*]

[a] *College of Food Science and Technology, Huazhong Agricultural University, Wuhan 430070, China*
[b] *Key Laboratory of Environment Correlative Food Science (Huazhong Agricultural University), Ministry of Education, Wuhan, China*

ARTICLE INFO

Article history:
Received 22 June 2016
Received in revised form
31 July 2016
Accepted 22 August 2016
Available online 3 November 2016

Keywords:
detoxicity
persimmon
phospholipase A_2
surface plasmon resonance

ABSTRACT

The effects of persimmon tannin (PT) characteristic structural elements on *Naja atra* phospholipase A_2 (PLA_2)-induced lethality, myotoxicity, and hemolysis in mice models were determined. In addition, methods including surface plasmon resonance, dynamic light scattering, and Fourier transform infrared spectroscopy were explored to uncover the possible detoxifying mechanisms of PT on snake venom PLA_2. Our results revealed that PT characteristic elements (EGCG, ECG, A-type EGCG dimer, and A-type ECG dimer) could neutralize the lethality, myotoxicity, and hemolysis of PLA_2. Moreover, the detoxifying effects of the four structural elements correlated with their structural disturbing effects well. Our results proved that A-type EGCG dimer and A-type ECG dimer may be structural requirements for the detoxifying effects of PT. We propose that the high affinity of A-type EGCG dimer and A-type ECG dimer for PLA_2 and the considerable spatial structural disturbance of PLA_2 induced by the dimers may be responsible for their antilethality, antimyotoxicity, and antihemolysis on Chinese cobra PLA_2 *in vivo*.

1. Introduction

Phospholipase A_2 (PLA_2, E.C. 3.1.1.4) from snake venoms displays numerous toxicities, such as neurotoxicity, cardiotoxicity, myotoxicity, edema, hemolysis, and anticoagulation [1]. Besides the well-known used antisera and chemical antidotes, plant polyphenols such as rosmarinic acid, myricetin, and aristolochic acid have been reported to be effective inhibitors of snake venoms [2]. Persimmon tannin (PT), which has a unique structure of high polymerization, high galloylation, and with both A and B type linkages and an unusual flavonol terminal unit [3], was reported to exhibit significant effects on improving the survival rate of mice injected with snake venom [4].

* *Corresponding author*. College of Food Science and Technology, Huazhong Agricultural University, Wuhan 430070, China.
E-mail addresses: lichmyl@126.com, lichmyl@mail.hzau.edu.cn (C.-M. Li).
http://dx.doi.org/10.1016/j.jfda.2016.08.005

Although the significant inhibition of PT on snake PLA_2 was confirmed in our previous study [5], and PT was also found to have higher affinity for PLA_2 than for BSA at physiological pH [6], detailed detoxifying mechanisms of PT were poorly understood because of the very complex structure of PT. To illustrate the antisnake PLA_2 mechanism of PT, the characteristic structural elements of PT were studied. The results showed that PT characteristic structural elements such as epigallocatechin-3-gallate-(4β→8, 2β→O→7)-epigallocatechin-3-gallate (A-type EGCG dimer) and epicatechin-3-gallate-(4β→8, 2β→O→7)-epicatechin-3-gallate (A-type ECG dimer) could potently inhibit the catalytic activity of PLA_2 *in vitro* [7]. However, it was reported that there was a dissociation of pharmacological effects and catalytic activity in snake PLA_2s [1], so changes in the enzymatic activity of PLA_2 *in vitro* could not represent the changes in toxicity of PLA_2 *in vivo*. In addition, considering that the detoxifying process of polyphenol on PLA_2 *in vivo* is a complex process, the structural disturbing effects of PT on PLA_2 obtained from a very short interaction period could not imitate the situation *in vivo*, which may need several to dozens of hours. Considering that ECG and EGCG are the main structural elements of PT, and A-type EGCG dimer and ECG dimer are characteristic structural elements of PT, in the present study, we therefore further compared the detoxifying effects of the four structural elements (Figure 1) on PLA_2 by determining the lethality, myotoxicity, and hemolysis of PLA_2 in mice models. Moreover, more methods including surface plasmon resonance (SPR), dynamic light scattering (DLS), and Fourier transform infrared spectroscopy (FT-IR) were used to explore their interaction after incubating the mixture for 24 hours. We believe that our current work extends our previous work and provides more detailed information on the action between PLA_2 and PT structural elements, which helps to improve our understanding of the detoxifying mechanism of PT *in vivo*.

2. Methods

2.1. Materials

Chinese cobra (*N. naja atra*) phospholipase A_2 (PLA_2, 9001-84-7) was purchased from ZhongXin DongTai Nano Gene Biotechnology Co. Ltd. (Laiyang, China) with a purity of more than 95% and a molecular weight of 13,260 Da. EGCG (purity ≥95%) and ECG (purity ≥95%) were purchased from Yuanye Bio-Technology Co. Ltd. (Shanghai, China). EGCG dimer (purity ≥90%) and ECG dimer (purity ≥90%) were separated from persimmon as we previously reported [3] and further purified by preparative high performance liquid chromatography (HPLC). Their purity and identity were confirmed by HPLC and mass spectrometry. All other chemicals were of analytical reagent grade, and Milli-Q water was used in all experiments.

2.2. Animals

Male Kunming mice (19 ± 2.13 g) were purchased from the Experimental Animal Center of Disease Prevention and Control of Hubei province (Wuhan, China). All animals were maintained under standard conditions (temperature, 22–25°C; humidity, 50–70%). All experiments were performed in compliance with the Functional evaluation program of health food and Chinese legislation on the use and care of laboratory animals.

2.3. Antilethality of PT structural elements

The median lethal dose (LD_{50}) of PLA_2 was determined by injecting different concentrations (25, 15, 10, 5, 2.5 mg/kg body weight) of venom at a constant volume of 0.2 mL/10 g body weight by intraperitoneal (i.p.) administration, and LD_{50} was calculated according to the method described by Theakston and Reid [8]. PLA_2 was incubated with or without PT characteristic elements (the molar ratio of PLA_2/phenol was 1:15) in pH 7.4 Tris–HCl buffer at 37°C for 24 hours. The ability of PT elements to inhibit the lethal action of PLA_2 was assessed by i.p. administration of $2LD_{50}$ of PLA_2 into groups ($n = 10$) of mice after starvation treatment for 12 hours. Meanwhile, the corresponding dose of PT elements was independently administered in the same manner. In all cases, the mice were observed for symptoms/signs of neurotoxicity, and the number of dead mice in each group was recorded.

2.4. Antimyonecrosis activities of PT structural elements

The potential ability of PT characteristic elements to inhibit PLA_2-induced myonecrosis was studied by intramuscular administration of 5 mg/kg body weight PLA_2 (incubated with or without PT elements at a molar ratio of 1:15 for 24 hours) to groups of mice ($n = 6$). The saline and corresponding dose of PT elements were independently administered in the same way. After 2 hours of administration, whole blood was collected from the mice eyes and allowed to clot for 1 hour. Later, the blood was centrifuged, and the serum was collected for experiment. CK kit (Nanjing Jiancheng) was used to determine creatine kinase (CK) levels in the mice serum.

2.5. Antihemolysis activities of PT structural elements

Indirect hemolysis was determined using the method described by Sharp et al [9] with several modifications. Briefly, the emulsified lecithin and 1 mg/mL PLA_2 (incubated with or without PT elements at a molar ratio of 1:15 for 24 hours) were incubated for 15 minutes at 37°C, then EDTA was added to terminate the interaction. The corresponding dose of PT characteristic elements, Tris–HCl buffer (negative control), and 1% Triton X-100 (positive control) were conducted in the same way. Then, 5% (v/v) mice erythrocytes were mixed with the above reaction system and incubated for 60 minutes at 37°C, followed by being centrifuged at 1500*g* for 10 minutes. The amount of hemoglobin released in the supernatant was estimated at 545 nm.

2.6. Surface plasmon resonance

PlexArray HT Biacore (Plexera, US) was used for SPR analysis. PT characteristic elements were printed in a photo-crosslinked chip by a photo-crosslinker system. The chip was washed with DMF, C_2H_5OH, and Milli-Q water and dried with nitrogen flow. Different concentrations (125nM, 250nM, 500nM, 1000nM, and 2000nM) of PLA_2 were used as analyte in

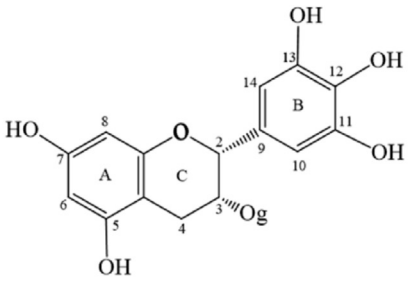

Epigallocatechin-3-gallate（EGCG）

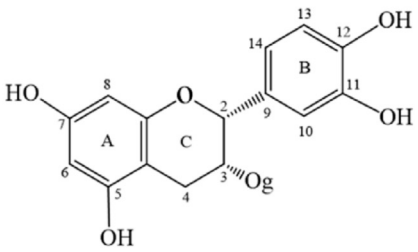

Epicatechin-3-gallate（ECG）

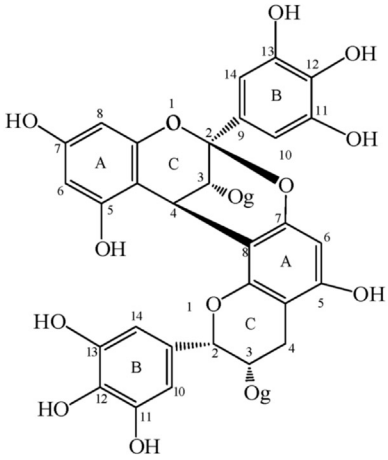

A-type EGCG dimers

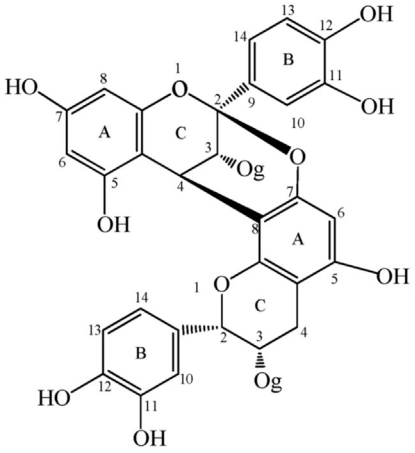

A-type ECG dimers

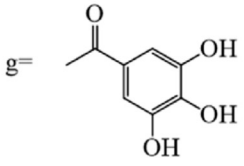

Figure 1 – Structures of the characteristic elements of persimmon tannin.

the fluid phase, with 50mM Tris–HCl (pH 7.4) as the running buffer. Both association and disassociation were performed at a flow rate of 2 μL/s for 300 seconds under 37°C. Then, 0.5% sodium dodecyl sulfate was used to regenerate the surface and remove bound proteins from the small molecules, enabling the sensor chip to be reused for additional analyte injections.

2.7. *Dynamic light scattering*

The particle size and zeta potential of PLA_2 were determined by DLS using Zetasizer Nano-ZS90 (Malvern Instruments Ltd., Malvern, UK). First, 0.7 mg/mL PLA_2 was incubated with PT elements in different molar ratios (PLA_2/phenol = 1:1, 1:10, 1:20, 1:30, 1:40, 1:50) at 37°C for 24 hours. Then size measurements were undertaken at 37°C in a quartz cell. The scattering angle was 173° backscatter. The refractive index of protein (1.45) and water (1.33) at 37°C was taken from the Zetasizer software.

2.8. *Fourier transform infrared spectroscopy*

The infrared spectra of PLA_2 was measured using a Nicolet Nexus 470 Fourier transform spectrophotometer (Nicolet, US) in the 400–4000 cm^{-1} range, with a resolution of 4 cm^{-1}. KBr was used as a reference. For each measurement, 128 scans were taken. PLA_2 (2.7 mg/mL) was incubated with PT elements at a molar ratio of 1:15 at 37°C for 24 hours, then the mixture

was dialyzed and lyophilized prior to the experiment. The corresponding dose of PT elements was conducted in the same way. The spectra of PLA_2-PT structural units were obtained by subtracting the spectrum of PT structural units-free form from that of PLA_2-PT structural unit complexes. The curve-fitting of 1700 to 1600 cm^{-1} (amide I) was performed using PeakFit 4.12 Software. The assignment of the bands in amide I region was in reference to Byler and Susi [10]. The peak area of each band was computed to calculate the contents of the secondary structures in PLA_2.

2.9. Statistical analysis

The results were expressed as the mean ± standard deviation, and statistical significance between the groups was determined using one-way analysis of variance test by IBM SPSS Statistics 19.0. A p value less than 0.05 was considered statistically significant.

3. Results

3.1. Antilethality activities of the four structural elements

The LD_{50} (i.p. injection) of PLA_2 calculated from the dose–response curve was 9.690 mg/kg body weight. As shown in Table 1, challenging the mice with $2LD_{50}$ dose of PLA_2 (i.p. injection) caused 100% lethality, and all mice died within 2–6 hours after injection. However, PT characteristic elements increased both the survival time and survival number of mice (Table 1). EGCG dimer and ECG dimer exhibited more potent antilethality than monomers, with 60% and 50% of survival rate, respectively, whereas only 20% and 10% of survival rate for EGCG and ECG, separately, were observed. It was observed that the mice that received PLA_2 alone showed typical toxic signs of tachypnea, hemiplegia, tremble, and akinesia, whereas all the surviving mice administered with PLA_2 that was incubated with PT characteristic elements developed none of these signs, and PT characteristic elements alone showed no lethal and neurotoxic toxicity in mice.

Table 1 – Effects of PT characteristic structural elements on the lethal toxicity of PLA_2.

	Number of mice	Number of dead mice	Survival ratio (%)	Time until death occurred (h)
PLA_2	10	10	0	2–6
PLA_2–EGCG	10	8	20	6–24
PLA_2–ECG	10	9	10	6–24
PLA_2–EGCG dimer	10	4	60	6–24
PLA_2–ECG dimer	10	5	50	6–24
EGCG	10	0	0	—
ECG	10	0	0	—
EGCG dimer	10	0	0	—
ECG dimer	10	0	0	—

ECG = epicatechin-3-gallate; EGCG = epigallocatechin-3-gallate; PLA_2 = phospholipase A_2; PT = persimmon tannin.

3.2. Antimyonecrosis activities of the four structural elements

The concentration of serum CK increased when there was necrosis in muscles [2]. Therefore, CK can be used as an enzymatic index of cellular myonecrosis damage. As shown in Figure 2, PT structural units did not induce myonecrosis as evidenced by the similar levels in CK enzyme activity with the normal group, whereas PLA_2 alone increased the CK level to about five times that of the normal group, indicating the high myotoxicity of PLA_2. However, PT characteristic elements significantly reduced the increased serum CK levels of PLA_2 poisoned mice, highlighting that PT structural units could significantly inhibit the myotoxicity of PLA_2. EGCG dimer and ECG dimer decreased the serum CK level of PLA_2 induced mice by about 60%, whereas EGCG and ECG lowered the serum CK level by about 40%, indicating the stronger antimyonecrosis activities of dimers than that of the monomers.

3.3. Antihemolysis activities of the four structural elements

As indicated in Figure 3, PT characteristic elements did not show any indirect hemolysis (<5%), whereas PLA_2 alone exhibited strong hemolytic activity, with a hemolysis ratio of 89.05 ± 3.90%. Both EGCG dimer and ECG dimer significantly decreased the indirect hemolytic activity of PLA_2 ($p < 0.05$), and 31.89 ± 2.54% and 29.61 ± 2.07% of neutralization were observed. In contrast, EGCG and ECG monomer exhibited little effects on inhibiting the hemolytic activity of PLA_2, wherein only 18.59 ± 4.62% and 19.23 ± 1.39% of neutralization were observed separately.

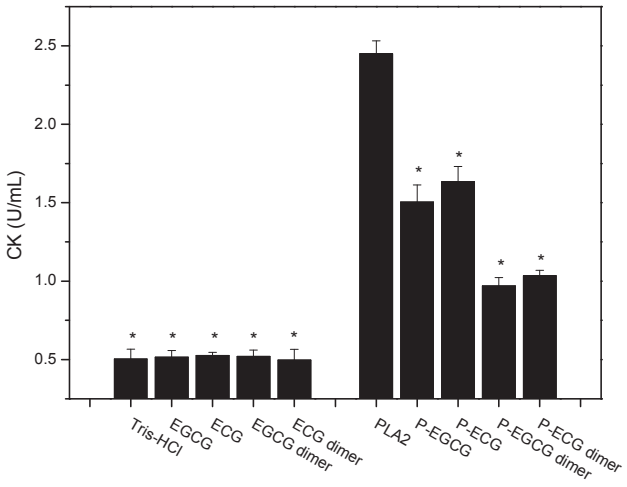

Figure 2 – Effects of persimmon tannin (PT) characteristic structural elements on the myotoxic activity induced by phospholipase A_2 (PLA_2) as measured by creatine kinase (CK) release. Data are expressed as means ± standard deviation ($n = 6$). *$p < 0.05$ as compared to the PLA_2 group.

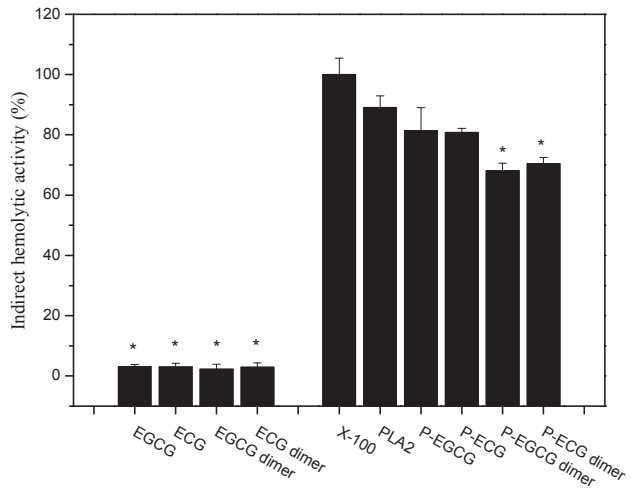

Figure 3 – Effects of PT characteristic structural elements on the indirect hemolytic activity of PLA_2. Data are expressed as means ± SD ($n = 6$). *$p < 0.05$ as compared to the PLA_2 group. PLA_2 = phospholipase A_2; PT = persimmon tannin; SD = standard deviation.

3.4. *Affinities of the four structural elements to PLA_2*

For SPR study, the surface of chip was stabilized with PT characteristic elements, and then various concentrations of PLA_2 were injected to the chip. As shown in Figure 4, signal response was observed after injecting the PLA_2 solution, indicating that the interaction occurred. And the interaction was enhanced with the increase of the PLA_2 concentration. Compared with EGCG and ECG monomers, EGCG and ECG dimer generated three times higher signal response with PLA_2, indicating that the interaction between PLA_2 and the dimers was stronger than that with the monomers.

Both association constant (K_a) and dissociation constant (K_d) could be obtained from the SPR curve by fitting the curve with Langmuir equation, and equilibrium dissociation constant (K_D) was calculated from K_a and K_d. As shown in Table 2, the K_D values of EGCG dimer and ECG dimer were 1.69×10^{-7}M and 1.78×10^{-7}M, respectively, whereas those of EGCG and ECG were 2.55×10^{-7}M and 3.34×10^{-7}M, separately, manifesting that the affinity of PT dimers to PLA_2 was higher than that of monomers.

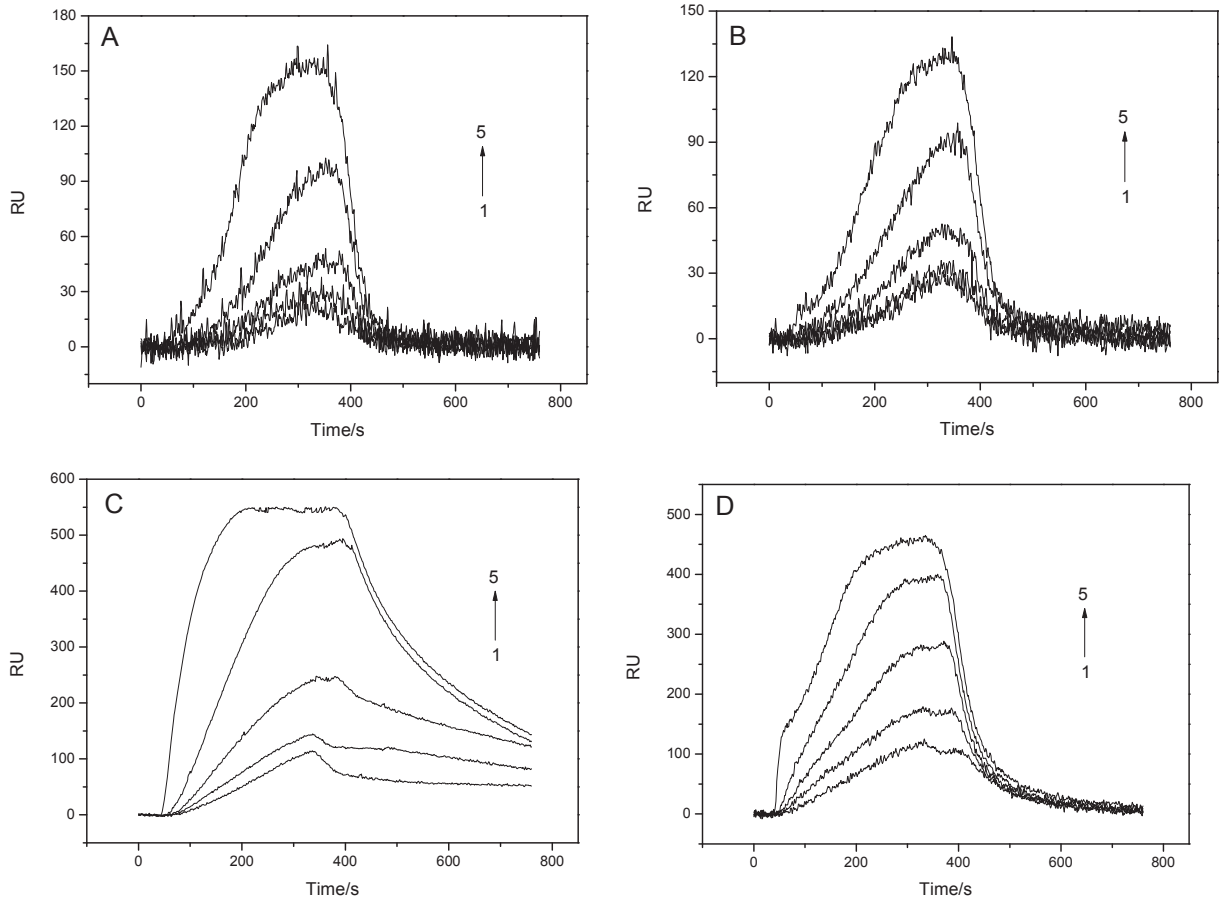

Figure 4 – The binding curves of PT characteristic structural elements with different concentration gradient of PLA_2. 1→5: 125nM, 250nM, 500nM, 1000nM, 2000nM. (A) EGC G. (B) ECG. (C) EGCG dimer. (D) ECG dimer. ECG = epicatechin-3-gallate; EGCG = epigallocatechin-3-gallate; PT = persimmon tannin.

Table 2 – Dynamic parameters of PT characteristic structural elements binding to PLA_2.

	K_a (1/Ms)	K_d (1/s)	K_D (M)
EGCG	4.99×10^2	1.27×10^{-4}	2.55×10^{-7}
ECG	1.82×10^3	6.07×10^{-4}	3.34×10^{-7}
EGCG dimer	9.81×10^3	1.66×10^{-3}	1.69×10^{-7}
ECG dimer	7.29×10^3	1.30×10^{-3}	1.78×10^{-7}

ECG = epicatechin-3-gallate; EGCG = epigallocatechin-3-gallate; PLA_2 = phospholipase A_2; PT = persimmon tannin.

3.5. *Diameters of PLA_2-PT structural elements*

The mean diameter of PLA_2 without polyphenols was 4.98 ± 0.18 nm. In the presence of PT characteristic elements, the mean size of PLA_2 continually increased with an increasing concentration of polyphenols (Table 3). As shown in Table 3, the PLA_2-dimer particles formed at high PLA_2/phenol ratios (above 1:20) were significantly larger than that of PLA_2-monomer particles. And it was noteworthy that EGCG dimer induced PLA_2 precipitated at the molar ratio of 1:40. Additionally, larger particle sizes were observed for EGCG dimer than for ECG dimer with PLA_2 at the same molar ratio.

3.6. *Effects of four structural elements on the secondary structure of PLA_2*

Among the numerous amide bands of the protein exhibited by FT-IR, the amide I band in the range of 1600–1700 cm^{-1} (representing C=O stretching/hydrogen bonding coupled with COO–) and the amide II band (representing NH bending coupled with C–N stretching) have been widely used in studying the secondary structure of protein [11]. As shown in Figure 5, native PLA_2 showed amide I peak at 1654 cm^{-1} and amide II peak at 1543 cm^{-1}. Upon binding with PT characteristic units, the amide I peak showed a significant blue shift from 1654 cm^{-1} to 1630 cm^{-1}, and 9 cm^{-1} of red shift (from 1543 cm^{-1} to 1552 cm^{-1}) was observed in the amide II band, indicating that PT structural units affected the secondary structures of PLA_2 significantly.

To compare the detailed secondary structure changes in PLA_2 after interacting with PT structural elements, amide I of the protein was analyzed using PeakFit software (Figure 6). Based on the curve-fitting of amide I, the secondary structural contents of PLA_2 were obtained. As indicated in Table 4, binding with PT structural units led to a decrease in α-helix and β-turn contents, accompanying an increase in β-sheet and random coil contents. But addition of different PT structural elements resulted in different degree changes in the secondary structure of PLA_2. EGCG and ECG dimers caused a decrease in the content of α-helix from 42.26% to about 14%, but an increase in β-sheet content from 14.27% to about 63%, whereas adding monomers to PLA_2 led to a decrease in α-helical content to about 18%, and an increase in β-sheet content to about 57%, manifesting that PT dimers affected the secondary structure of PLA_2 more substantially.

4. Discussion

Plant extracts have been traditionally used in the treatment of snakebite envenomations in many countries, especially in rural areas where antivenin is not readily available. Phenolic compounds were one of the main classes of plant extracts that could inhibit snake venoms [12]. Our previous study [7] showed that the PT characteristic elements could inhibit the catalytic activity of PLA_2 potently, and to explore whether the main structural elements and the characteristic structural units of PT could also inhibit the toxicity of PLA_2, the animal experiments were conducted. Our current data suggested that all four structural elements showed detoxifying effects on PLA_2, but A-type EGCG and ECG dimer exerted significantly more potent antilethality, antimyonecrosis, and antihemolysis activities than EGCG and ECG. It was confirmed that the characteristic elements of A-type EGCG and ECG dimer units might also play a vital role in neutralizing the myotoxicity, hemolysis, and lethality of snake venom PLA_2, which extended our previous study. Because both A and B type linkages are exited in PT, it is meaningful to compare the biological activities as well as structural disturbing effects of A type and B type EGCG and ECG dimers on PLA_2. Unfortunately, we were unable to obtain the B type EGCG and ECG dimers from PT, despite our numerous attempts. The preparation of B type dimers of EGCG and ECG is a challenging task, and it requires further work.

It was suggested that phenolic compounds could form complexes with zymoprotein, thus exhibiting the enzyme inhibitory activity [13]. To investigate whether the antitoxic effect of PT structural elements on PLA_2 was correlated with their binding with PLA_2, we first compared the binding affinities of PT characteristic units to PLA_2 using the SPR method. The results showed that PT dimers showed higher affinities to PLA_2 than monomers. However, the SPR method only permits the determination of the interaction between the PT structural elements with PLA_2 in a very short contacting period.

Table 3 – Particle size of PLA_2 prior to and after interacting with PT characteristic structural elements.

Molar ratio (PLA_2/phenol)	PLA_2–EGCG	PLA_2–ECG	PLA_2–EGCG dimer	PLA_2–ECG dimer
1:0	4.98 ± 0.18	4.98 ± 0.18	4.98 ± 0.18	4.98 ± 0.18
1:1	5.94 ± 0.09	4.73 ± 0.45	6.36 ± 0.32	6.10 ± 0.35
1:10	8.42 ± 0.14	5.94 ± 0.13	8.02 ± 0.11	7.67 ± 0.72
1:20	9.90 ± 0.44	6.88 ± 0.17	1276.48 ± 37.10	1017.87 ± 45.36
1:30	36.50 ± 2.27	13.45 ± 0.74	2303.33 ± 67.04	2132.67 ± 277.80
1:40	525.33 ± 44.34	19.01 ± 4.17	—	2257.33 ± 142.38

ECG = epicatechin-3-gallate; EGCG = epigallocatechin-3-gallate; PLA_2 = phospholipase A_2; PT = persimmon tannin.

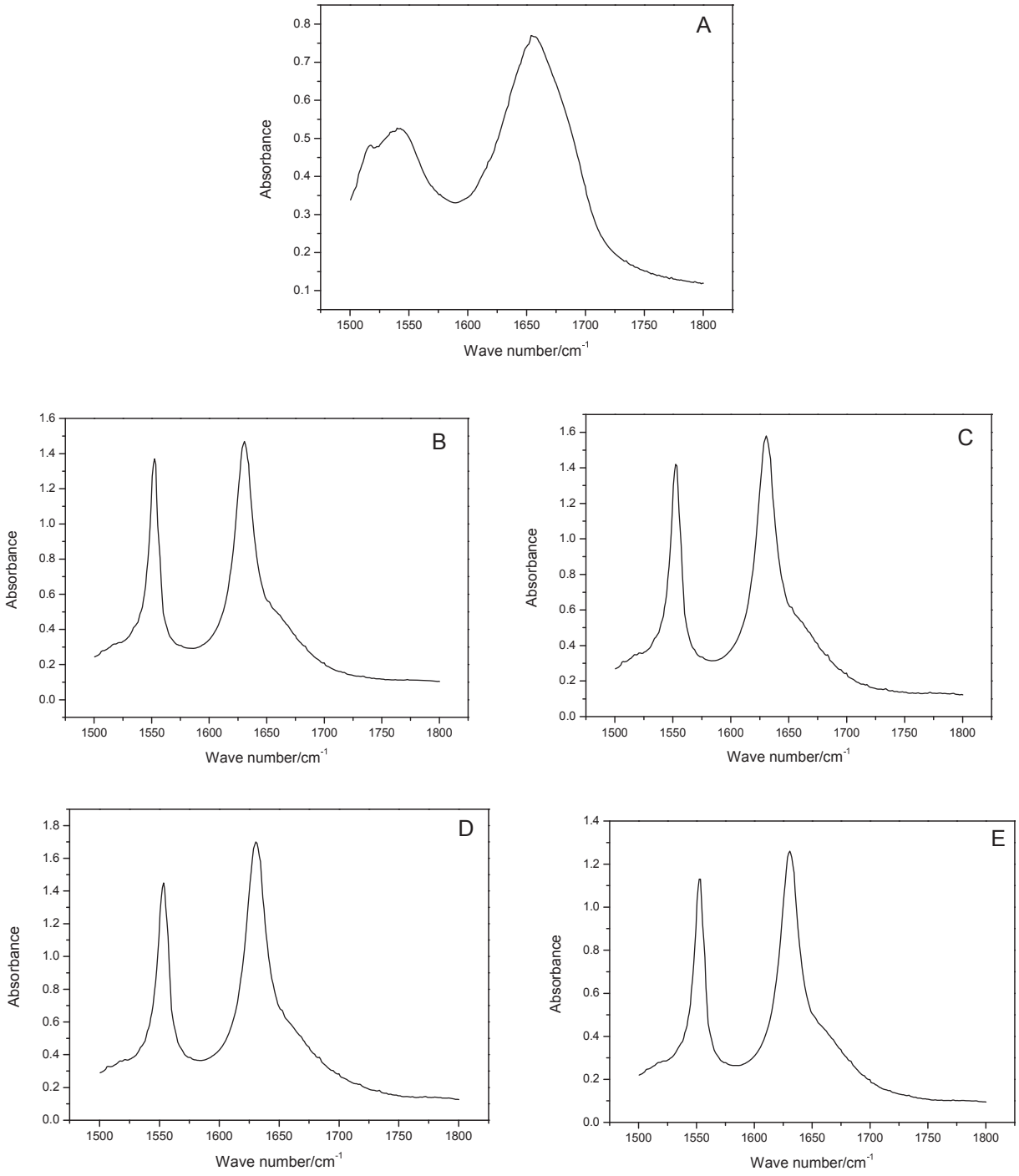

Figure 5 – FT-IR spectra (1500–1800 cm^{-1}) of PLA_2 prior to and after interacting with PT characteristic structural elements. (A) PLA_2. (B) PLA_2–EGCG. (C) PLA_2–ECG. (D) PLA_2–EGCG dimer. (E) PLA_2–ECG dimer. ECG = epicatechin-3-gallate; EGCG = epigallocatechin-3-gallate; FT-IR = Fourier transform infrared spectroscopy; PLA_2 = phospholipase A_2; PT = persimmon tannin.

Considering that the interaction of polyphenol on PLA_2 *in vivo* is a complex process, which may last several to dozens of hours, we further prolonged the incubation time of PT structural elements and PLA_2 to 24 hours, and detected the particle size changes of PLA_2 after interacting with PT structural units by DLS methods. The increasing diameter of PLA_2 after interacting with PT structural units indicated that complexes were formed between them [14]. The difference in the complex size referred to a difference in the binding affinity between protein and polyphenols [15]. PT dimers showed higher affinities to PLA_2 than monomers as expressed by larger particle sizes, which was in line with SPR results. The higher

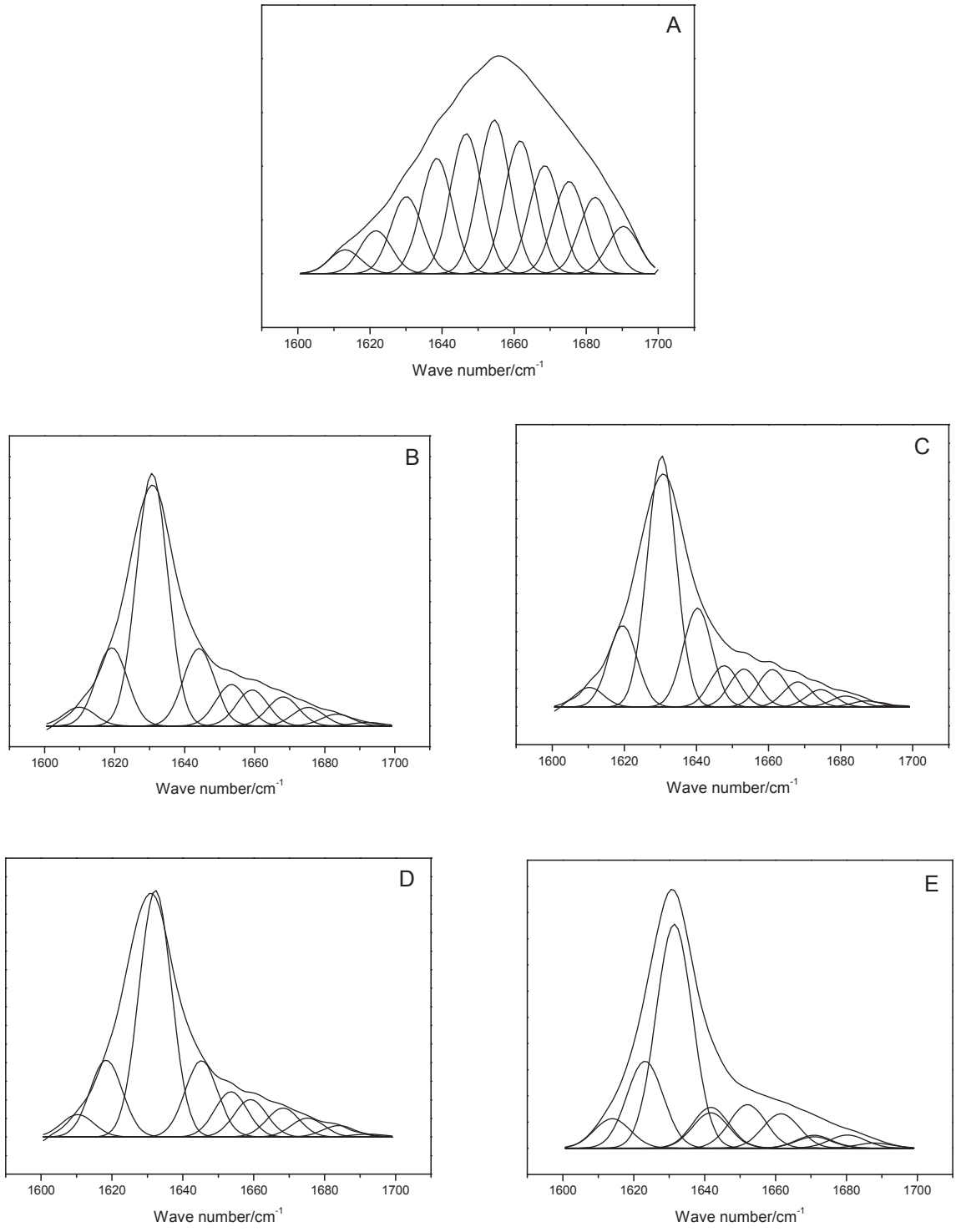

Figure 6 – IR fitting spectra of amide I band of PLA_2 prior to and after interacting with PT characteristic structural elements. (A) PLA_2. (B) PLA_2–EGCG. (C) PLA_2–ECG. (D) PLA_2–EGCG dimer. (E) PLA_2–ECG dimer. ECG = epicatechin-3-gallate; EGCG = epigallocatechin-3-gallate; IR = infrared; PLA_2 = phospholipase A_2; PT = persimmon tannin.

affinities of EGCG and ECG dimer to PLA_2 than that of ECG and EGCG monomers could be explained by the higher molecular weight, the more orthophenolic groups and gallate moieties, as well as the more elongated structure of the former compared with the latter [16]. When paralleling the order of the affinity of the four PT structural elements to PLA_2 with their detoxifying effects on PLA_2, we found a very similar tendency, indicating that the antitoxic effect of PT structural elements on PLA_2 might correlate with their binding with PLA_2.

Table 4 – Effects of PT characteristic elements on the secondary structures of PLA_2.

	Content of secondary structure of PLA_2 (%)			
	β-sheet	Random coil	α-helix	β-turn
PLA_2	14.27	11.43	42.26	32.10
PLA_2–EGCG	58.30	14.12	16.12	11.46
PLA_2–ECG	56.55	14.26	19.14	10.04
PLA_2–EGCG dimer	63.46	14.31	14.19	8.03
PLA_2–ECG dimer	63.31	14.18	14.56	7.96

ECG = epicatechin-3-gallate; EGCG = epigallocatechin-3-gallate; PLA_2 = phospholipase A_2; PT = persimmon tannin.

The toxicity of PLA_2 was highly correlated with its spatial structure. In order to illustrate whether the detoxifying effects of PT structural elements correlated with their effects on the structural changes of PLA_2, the secondary structural changes of PLA_2 prior to and after interacting with PT structural units for 24 hours were determined.

Previously, we observed that after incubating with PT elements for 30 minutes, the α-helix content of PLA_2 increased significantly and the β-sheet content of PLA_2 decreased notably [7]. However, a significant decrease in the α-helix content and a notable increase in the β-sheet content of PLA_2 were observed by FT-IR analysis in the current study after extending the incubation time from 30 minutes to 24 hours. It is well known that the interaction between protein and polyphenol is a very complex process and can be affected by numerous factors such as the concentrations of both protein and polyphenol, the ionic strength and pH value of the solution, and the incubation time and temperatures. A slight change in the influencing factor might affect the nature of the interaction between protein and polyphenol [17]. The inconsistent results can be explained by the following reasons. First, because polyphenols were prone to oxidation under neutral or basic conditions in the presence of oxygen [18], prolonging the incubation time from 30 minutes to 24 hours in the current study led to the nonenzymatic oxidation of polyphenols, thus resulting in different secondary structural disturbing effects on PLA_2. Second, during the long period of incubation, molecules of polyphenol or PLA_2 or the polyphenol–PLA_2 complex would undergo rearrangement and self-aggregation, thus exerting structural disturbing effects on PLA_2 that are distinct from those of short-time incubation. Our results suggest that the interaction modes of polyphenols–proteins were not only structure and concentration dependent, but also incubation time dependent. Because the detoxifying process of polyphenol on PLA_2 *in vivo* is a complex process, when elucidating the detoxifying mechanism of polyphenols in the view of the interaction between polyphenols and snake venom, both the existing state of polyphenols under physiological conditions and the interaction time should be considered.

Comprehensively, the four PT structural elements induced conformational and secondary structural changes in PLA_2, of which A-type EGCG and ECG dimer exerted more potent effects on PLA_2 compared with EGCG and ECG. The results were in line with their detoxifying effects on PLA_2, indicating that the spatial structure change of PLA_2 induced by PT elements was probably one of the detoxifying mechanisms of PT.

His48 was reported to be highly conserved in PLA_2, and this residue was essential for the phospholipid hydrolysis activity of PLA_2 [19]. Some pharmacological activities, such as myotoxic, cytotoxic, and hemolytic activities, were probably dependent on the integrity of the catalytic activity [20]. So His was also a key residue in the lethal, myotoxic, and hemolytic activities of PLA_2 aside from the enzymatic activity. Although Lys was reported to be irrelevant to the enzymatic activity of *N. atra* PLA_2, the residue played an important role in lethality as well as anticoagulant, hemolytic, and myotoxic activities [21]. Moreover, Trp in *N. atra* PLA_2 was identified to be not specifically associated with the enzymatic sites or the toxic sites, but still had some relationship with both activities [22]. Another active residue in *N. atra* PLA_2 was Tyr (Tyr3 and Tyr63), which showed important effects on the lethal potency of snake venom [23]. From the secondary structure of *N. atra* PLA_2 [24], it was found that His48, Lys6, Lys115, Trp18, Trp19, and Tyr3 were located in the α-helical structures, whereas Lys56, Lys65, and Tyr63 were located in the β-turn structures. Interestingly, our study showed that PT characteristic elements could decrease both the α-helix and β-turn contents of PLA_2, implying that PT units probably affected the environment of the critical residues, such as His, Lys, Trp, and Tyr, of PLA_2, thus reducing the toxicity of PLA_2. A-type EGCG and ECG dimer affected the secondary structure of PLA_2 more severely, accompanied with stronger effects on the environment of key residues, hence exerting more potent detoxifying capacities than EGCG and ECG.

To conclude, PT characteristic elements (EGCG, ECG, EGCG dimer, and ECG dimer) showed significant neutralizing effects on the myotoxicity, hemolysis, and lethality of Chinese cobra PLA_2. And the detoxifying effects of the four structural elements correlated with their structural disturbing effects well. Our results also suggested that the secondary structure changes of proteins taking place when mixing them with polyphenols differed with the incubation time. Therefore, the interaction time should be considered when elucidating the detoxifying mechanism of polyphenols in view of the interaction between polyphenols and snake venom. Our current work extends our previous work and helps us better understand the antivenom mechanism of PT *in vivo*.

Conflicts of interest

The authors declare that there are no conflicts of interest.

Acknowledgments

This work was supported by the National Natural Science Foundation of China (grant number 31271833).

REFERENCES

[1] Soares AM, Giglio JR. Chemical modifications of phospholipases A2 from snake venoms: effects on catalytic and pharmacological properties. Toxicon 2003;42:855–68.

[2] Shenoy PA, Nipate SS, Sonpetkar JM, Salvi NC, Waghmare AB, Chaudhari PD. Anti-snake venom activities of ethanolic extract of fruits of *Piper longum* L. (Piperaceae) against Russell's viper venom: characterization of piperine as active principle. J Ethnopharmacol 2013;147:373–82.
[3] Li C, Leverence R, Trombley JD, Xu S, Yang J, Tian Y, Reed JD, Hagerman AE. High molecular weight persimmon (*Diospyros kaki* L.) proanthocyanidin: a highly galloylated, A-linked tannin with an unusual flavonol terminal unit, myricetin. J Agric Food Chem 2010;58:9033–42.
[4] Okonogi T, Hattori Z, Ogiso A, Mitsui S. Detoxification by persimmon tannin of snake venoms and bacterial toxins. Toxicon 1979;17:524–7.
[5] Xu S-F, Zou B, Yang J, Yao P, Li C-M. Characterization of a highly polymeric proanthocyanidin fraction from persimmon pulp with strong Chinese cobra PLA2 inhibition effects. Fitoterapia 2012;83:153–60.
[6] Li C-M, Zhang Y, Yang J, Zou B, Dong X-Q, Hagerman AE. The interaction of a polymeric persimmon proanthocyanidin fraction with Chinese cobra PLA2 and BSA. Toxicon 2013;67:71–9.
[7] Zhang Y, Zhong L, Zhou B, Chen J-Y, Li C-M. Interaction of characteristic structural elements of persimmon tannin with Chinese cobra PLA 2. Toxicon 2013;74:34–43.
[8] Theakston RDG, Reid HA. Development of simple standard assay procedures for the characterization of snake venoms. B World Health Organ 1983;61:949–56.
[9] Sharp PJ, Berry SL, Spence I, Howden MEH. A basic phospholipase A from the venom of the australian king brown snake (*Pseudechis australis*) showing diverse activities against membranes. Comp Biochem Physiol B Biochem Biol 1989;92:501–8.
[10] Byler DM, Susi H. Examination of the secondary structure of proteins by deconvolved FTIR spectra. Biopolymers 1986;25:469–87.
[11] Surewicz WK, Mantsch HH, Chapman D. Determination of protein secondary structure by Fourier transform infrared spectroscopy: a critical assessment. Biochemistry 1993;32:389–94.
[12] Gopi K, Renu K, Sannanaik Vishwanath B, Jayaraman G. Protective effect of *Euphorbia hirta* and its components against snake venom induced lethality. J Ethnopharmacol 2015;165:180–90.
[13] Song H, Chen C, Zhao S, Ge F, Liu D, Shi D, Zhang T. Interaction of gallic acid with trypsin analyzed by spectroscopy. J Food Drug Anal 2015;23:234–42.
[14] Thongkaew C, Gibis M, Hinrichs J, Weiss J. Polyphenol interactions with whey protein isolate and whey protein isolate–pectin coacervates. Food Hydrocolloid 2014;41:103–12.
[15] Naczk M, Oickle D, Pink D, Shahidi F. Protein precipitating capacity of crude canola tannins: effect of pH, tannin, and protein concentrations. J Agric Food Chem 1996;44:2144–8.
[16] Poncet-Legrand C, Doco T, Williams P, Vernhet A. Inhibition of grape seed tannin aggregation by wine mannoproteins: effect of polysaccharide molecular weight. Am J Enol Viticult 2007;58:87–91.
[17] Ozdal T, Capanoglu E, Altay F. A review on protein–phenolic interactions and associated changes. Food Res Int 2013;51:954–70.
[18] Cilliers JJ, Singleton VL. Characterization of the products of nonenzymic autoxidative phenolic reactions in a caffeic acid model system. J Agric Food Chem 1991;39:1298–303.
[19] Andrião-Escarso SH, Soares AM, Rodrigues VM, Angulo Y, Díaz C, Lomonte B, Gutiérrez JM, Giglio JR. Myotoxic phospholipases A2 in Bothrops snake venoms: Effect of chemical modifications on the enzymatic and pharmacological properties of bothropstoxins from *Bothrops jararacussu*. Biochimie 2000;82:755–63.
[20] Fuly AL, Calil-Elias S, Martinez AMB, Melo PA, Guimarães JA. Myotoxicity induced by an acidic Asp-49 phospholipase A2 isolated from *Lachesis muta* snake venom: comparison with lysophosphatidylcholine. Int J Biochem Cell B 2003;35:1470–81.
[21] Condrea E, Rapuano BE, Fletcher JE, Yang C-C, Rosenberg P. Ethoxyformylation and guanidination of snake venom phospholipases A2: effects on enzymatic activity, lethality and some pharmacological properties. Toxicon 1983;21:209–18.
[22] Condrea E, Soons KR, Barrington PL, Yang C-C, Rosenberg P. Effect of alkylation of tryptophan residues on the enzymatic and pharmacological properties of snake venom phospholipase A2. Can J Physiol Pharm 1985;63:331–9.
[23] Soons KR, Condrea E, Yang C-C, Rosenberg P. Effects of modification of tyrosines 3 and 62(63) on enzymatic and toxicological properties of phospholipases A2 from *Naja nigricollis* and *Naja naja atra* snake venoms. Toxicon 1986;24:679–93.
[24] White SP, Scott DL, Otwinowski Z, Gelb MH, Sigler PB. Crystal structure of cobra-venom phospholipase A2 in a complex with a transition-state analogue. Science 1990;250:1560–3.